Check for updates

Wastewater treatment from the biodiesel production using waste cooking oil by electrocoagulation: a multivariate approach

Hanife Sari-Erkan

ABSTRACT

This study mainly focuses on the process of electrocoagulation (EC) for the wastewater treatment from biodiesel production using waste cooking oil. The effects of current density, initial pH and electrolysis time on the EC process using aluminum (Al) and iron (Fe) electrodes were investigated for removal of chemical oxygen demand (COD). The COD removal efficiencies were found to be 62.7% and 63.4% at optimum conditions for Al (current density: 43 mA/cm^2, pH: 5, time: 21 min) and Fe (current density: 47 mA/cm^2, pH: 7.7, time: 30 min) electrodes, respectively. At these optimum conditions, the removal efficiencies of oil & grease, total phosphorus (TP), orthophosphate (PO4-P) and total suspended solids (TSS) were determined respectively to be above 89.9%, 98.9%, 99.5%, 86.7% for Al electrodes and 90.8%, 98.5%, 97.6%, 89.6% for Fe electrodes. Total operating costs were also found to be 6.43 €/m^3 and 7.01 €/m^3 for Al and Fe electrodes, respectively. The results indicate that the EC process using both types of electrodes seems to ensure an efficient treatment of biodiesel wastewater in terms of oil & grease and TP.

Key words | biodiesel wastewater, cost analysis, electrocoagulation, optimization, response surface method (RSM), sludge properties

Hanife Sari-Erkan
Civil Engineering Faculty, Environmental Engineering Department,
Yildiz Technical University,
34220 Davutpasa, Esenler, Istanbul,
Turkey
E-mail: *hsari@yildiz.edu.tr*

INTRODUCTION

Biodiesel, one of the most attractive and promising alternative fuels, has been categorized among renewable resources and is currently being developed all over the world (Yaakob *et al.* 2013; Daud *et al.* 2015). Biodiesel has been preferred as an alternative energy resource because of its desirable chemical properties such as biodegradability, non-toxicity and carbon neutrality (Omar & Amin 2011; Tan *et al.* 2011). Carbon neutral fuels absorb carbon dioxide as they grow, and when burned, the same carbon is released back into the atmosphere (Mathews 2008). From an environmental perspective, biodiesel is considered 'carbon neutral' because all CO_2 released during consumption is removed from the atmosphere for the growth of vegetable oil plants (Barnwal & Sharma 2005). It also produces low nitrogen, carbon dioxide, sulfur, lead and hydrocarbon emissions in comparison to other non-renewable fuels such as petroleum or diesel, and this ensures a positive impact on the environment (Demirbas 2009).

Four main techniques may be used in biodiesel production: direct use and raw oil blending, pyrolysis, micro-emulsions and transesterification using edible oils, non-edible oils and reusable wastes such as feedstock (Vyas *et al.* 2010; Daud *et al.* 2015). Nowadays, transesterification is a common method for producing biodiesel (Siddiquee & Rohani 2011; Abbaszaadeh *et al.* 2012). The use of edible oils in biodiesel production can cause a food crisis and unnecessary clearing of forests for plantation (Chen *et al.* 2009; Talebian-Kiakalaieh *et al.* 2013). Therefore, many researchers have focused on waste cooking oils (WCO) and non-edible oils such as algae, microalgae and jatropha oils (Ganapathy *et al.* 2009; Abou-Shanab *et al.* 2011; Karatay & Dönmez 2011). WCO from homes and restaurants can be used in production of biodiesel to reduce water pollution and prevent blockages in water drainage systems (Yaakob *et al.* 2013). The use of WCO in biodiesel production can also reduce the costs of biodiesel production by 60–90% (Marchetti *et al.* 2008; Daud *et al.* 2015).

In the biodiesel production process, wastewater is mainly generated by the washing stage. The amount of wastewater produced by the washing process is high

doi: 10.2166/wst.2019.238

Downloaded from http://iwaponline.com/wst/article-pdf/79/12/2366/620291/wst079122366.pdf
by guest

(approximately 20–120 L of wastewater/100 L biodiesel) (Suehara *et al.* 2005; Srirangsan *et al.* 2009). Biodiesel wastewater is characterized by high chemical oxygen demand (COD), suspended solids (SS) and oil & grease. It is viscous wastewater with an opaque white color (Jaruwat *et al.* 2010; Rattanapan *et al.* 2011; Ramírez *et al.* 2012). Discharge of untreated biodiesel wastewater into public sewage systems leads to plugging of the pipe systems due to the high concentration of oil & grease. It might also affect the microbial activity of activated sludge in biological wastewater treatment plants (Daud *et al.* 2015). Individual biodiesel wastewater treatment methods have been employed for the removal of COD, SS and oil & grease, including coagulation (Kumjadpai *et al.* 2011; Ngamlerdpokin *et al.* 2011; Xie *et al.* 2011), electrocoagulation (Chavalparit & Ongwandee 2009; Srirangsan *et al.* 2009; Ngamlerdpokin *et al.* 2011; Sandhwar & Prasad 2018), adsorption (Pitakpoolsil & Hunsom 2013), biological processes (Suehara *et al.* 2005; Ramírez *et al.* 2012), and microbial fuel cell systems (Sukkasem *et al.* 2011).

Electrocoagulation (EC) is one of the attractive electrochemical treatment methods for biodiesel wastewater. EC is also reported as an alternative to chemical coagulation and a cost-effective treatment method because it reduces the usage of chemical coagulants (Butler *et al.* 2011). This treatment method has several advantages such as simple and rapid operation, requirement for lower or no chemical usage and lower treatment time (Un *et al.* 2009). It also generates smaller sludge amounts and leads to rapid precipitation of sludge flocs produced (Butler *et al.* 2011). Three main mechanisms, electrode oxidation, gas bubble generation and flotation or sedimentation of flocs, come into play in the EC process (Emamjomeh & Sivakumar 2009). The oxidation reactions that occur on the sacrificial electrode depend on the anode material (Al-Qodah & Al-Shannag 2017). Metallic hydroxide flocs are produced by electrodissolution of anodes, which are usually made of iron or aluminum in the EC process. On the other hand, production of H_2 occurs at the cathodes. In the EC process, destabilization of the dissolved pollutants in wastewater takes place, and aggregates emerge as the produced ferric hydroxide serves as coagulant (Al-Shannag *et al.* 2015). The main chemical reactions for Fe electrodes can be summarized as follows in basic conditions (Equations (1)–(4)) and acidic conditions (Equations (5)–(8)):

$$\text{Anode: } Fe(s) \rightarrow Fe^{2+}(aq) + 2e^- \quad (1)$$

$$\text{Cathode: } 2H_2O + 2e^- \rightarrow H_2(g) + 2OH^-(aq) \quad (2)$$

$$\text{Precipitation: } Fe^{2+}(aq) + 2HO^-(aq) \rightarrow Fe(OH)_2(s)\downarrow \quad (3)$$

$$\text{Overall: } Fe(s) + 2H_2O \rightarrow Fe(OH)_2(s)\downarrow + H_2(g) \quad (4)$$

$$\text{Anode: } 4Fe(s) \rightarrow 4Fe^{2+}(aq) + 8e^- \quad (5)$$

$$\text{Precipitation: } 4Fe^{2+}(s) + 10H_2O + 10O_2(g) \rightarrow 4Fe(OH)_3(s)\downarrow + 8H^+(aq) \quad (6)$$

$$\text{Cathode: } 8H^+(aq) + 8e^-(aq) \rightarrow 4H_2(g) \quad (7)$$

$$\text{Overall: } 4Fe(s) + 10H_2O + 10O_2(g) \rightarrow 4Fe(OH)_3(s)\downarrow + 4H_2(g) \quad (8)$$

The redox reactions for aluminum electrode systems may be summarized as the following equations in basic conditions (Equations (9)–(12)) and acidic conditions (Equations (13)–(16)):

$$\text{Anode: } Al(s) \rightarrow Al^{3+}(aq) + 3e^- \quad (9)$$

$$\text{Cathode: } 3H_2O + 3e^- \rightarrow 1.5H_2(g) + 3OH^-(aq) \quad (10)$$

$$\text{Precipitation: } Al^{3+}(aq) + 3HO^-(aq) \rightarrow Al(OH)_3(s)\downarrow \quad (11)$$

$$\text{Overall: } Al(s) + 3H_2O \rightarrow Al(OH)_3(s)\downarrow + 1.5H_2(g) \quad (12)$$

$$\text{Anode: } Al(s) \rightarrow Al^{3+}(aq) + 3e^- \quad (13)$$

$$\text{Precipitation: } Al^{3+}(aq) + 3H_2O \rightarrow Al(OH)_3(s)\downarrow + 3H^+(aq) \quad (14)$$

$$\text{Cathode: } 3H^+(aq) + 3e^- \rightarrow 1.5H_2(g) \quad (15)$$

$$\text{Overall: } Al(s) + 3H_2O \rightarrow Al(OH)_3(s)\downarrow + 1.5H_2(g) \quad (16)$$

As shown in Equations (9)–(16), as Al^{+3} is generated it reacts with hydroxyl to form $Al(OH)_2^+$ at low pH. Then, as pH increases, $Al(OH)_3$ is polymerized to form $Al_n(OH)_{3n}$ (Al-Qodah & Al-Shannag 2017).

The EC process is affected by several parameters such as initial current density, pH, reaction time and types of sacrificial electrodes. Treatment efficiency might also affect wastewater type (Butler *et al.* 2011). The EC process has been successfully applied to different types of wastewater. However, there are only a few studies that have investigated biodiesel wastewater treatment using the EC process so far.

This study investigated the treatability of biodiesel wastewater by the EC process using aluminum and iron electrodes with the addition of NaCl as an electrolyte solution. The effectiveness of the EC process using each electrode material for the treatment of biodiesel wastewater was evaluated and optimized in terms of removal efficiency. The approach of response surface method (RSM) using the central composite design (CCD) was chosen to improve a

Downloaded from http://iwaponline.com/wst/article-pdf/79/12/2366/620291/wst079122366.pdf
by guest

model and determine the process parameters' interactive effects. Cost analyses of the EC process and characteristics of waste sludge were also determined at the optimum operating conditions.

MATERIALS AND METHODS

Characterization of biodiesel wastewater

In this study, the biodiesel wastewater was taken from a small-scale biodiesel production plant in the province of Istanbul in Turkey. In this plant, waste cooking oil is used as feedstock, and the transesterification process is employed for biodiesel production. The main source of the wastewater was from the washing process. The biodiesel wastewater characteristics are shown in Table 1. The wastewater had 29,550 mg/L COD and 3.72 mS/cm conductivity at 20 °C. The pH of the raw biodiesel wastewater was 4.82.

Experimental procedure and measurements

The schematic presentation of the experimental set-up is shown in Figure 1. A laboratory-scale plexiglass EC reactor was used, with a 9-cm diameter and 13-cm height. The aluminum and iron electrodes (one anode and one cathode; Al-Al and Fe-Fe) were used as the sacrificial electrodes with dimensions of 11.5 cm height, 6 cm width and 0.1 cm thickness. In the optimization experiments, the effective electrode area and distance between the electrodes were 62.2 cm^2 and 2 cm, respectively. The electrodes were connected to a digital DC power supply (ADC-3306D) to impose the current in the laboratory experiments.

The test volume of biodiesel wastewater for each run was 400 mL. The laboratory experiments were performed under the operating conditions of 16 to 80 mA/cm^2 current density, pH 5–9 and 10–30 reaction time. The initial pH was adjusted using H_2SO_4 (6 N) and NaOH (6 N) solutions to reach the desired values. An electrolyte solution (NaCl: 4.5 g/L wastewater) was used, as the electrical conductivity of wastewater was not found to be sufficient for the EC process. As is known, the current efficiency will decrease when the electrolytic conductivity is low and generally NaCl is added in order to increase the electrolytic conductivity (Liu *et al.* 2010). Analyses were conducted by taking the supernatant from the reactor at the end of the settling process (180 min) after each run.

Table 1 | Biodiesel wastewater characteristics

Parameter	Mean value
pH	4.82
Electrical conductivity, (mS/cm)	3.72
COD (mg/L)	29,550 ± 1,035
Oil & grease (mg/L)	2,319 ± 36
TSS (mg/L)	1,564 ± 28
Total phosphorus (mg/L)	205.6 ± 12
Orthophosphate (mg/L)	93.9 ± 5

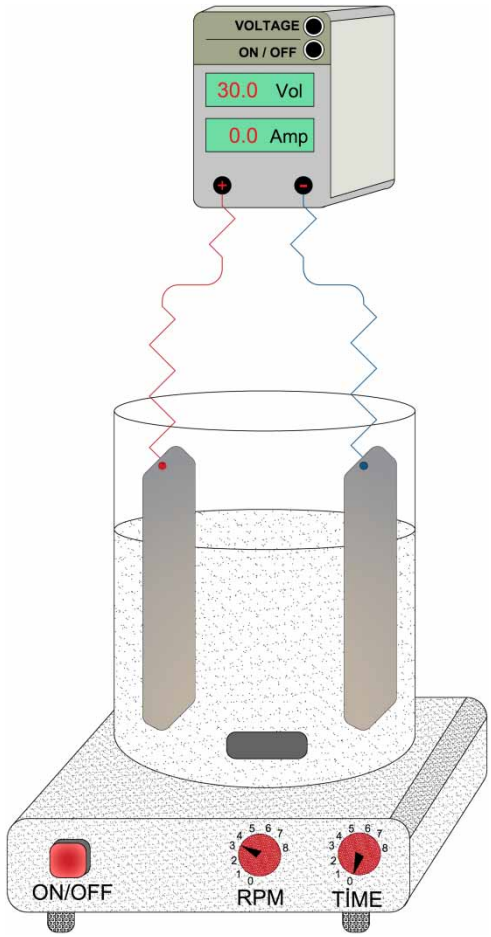


Figure 1 | Schematic presentation of EC process.

The analyses of COD, TSS, orthophosphate, oil & grease and chloride were carried out in accordance with *Standard Methods* (APHA 2005), and all the chemicals used in this study were of analytical-reagent grade. The sludge scanning electron microscopy (SEM) and Fourier transform infrared spectroscopy (FT-IR) analyses were performed to identify the sludge characterization using the Zeiss EVO® LS 10 and Perkin Elmer Spectrum 100 Fourier Transform Infrared Spectrophotometer, respectively.

Downloaded from http://iwaponline.com/wst/article-pdf/79/12/2366/620291/wst079122366.pdf
by guest

Experimental design and model development

In the study, the CCD, a powerful experimental design for RSM, was used to determine the individual and interactive effects of the EC process parameters (current density, initial pH and electrolysis time) on COD removal efficiencies of biodiesel wastewater using the Statgraphics Centurion XVII software. Current density (X_1), initial pH (X_2) and electrolysis time (X_3) were chosen as the independent process factors, while COD removal efficiencies (Y_1 and Y_2 for aluminum and iron electrodes respectively) were selected as the response parameters. As shown in Table 2, the ranges of the process variables were divided into three levels (−1, 0, +1). Second order polynomial equations were fitted to analyze the relationship between the process and response variables based on Equation (17).

$$Y = \beta_0 + \beta_1 X_1 + \beta_2 X_2 + \beta_3 X_3 + \beta_{11} X_1^2 + \beta_{22} X_2^2 + \beta_{33} X_3^2 + \beta_{12} X_1 X_2 + \beta_{13} X_1 X_3 + \beta_{23} X_2 X_3 \quad (17)$$

where β_0 is a constant, β_1, β_2 and β_3 are first-order model coefficients, β_{12}, β_{13}, β_{23} are interaction and β_{11}, β_{22}, β_{33} are squared coefficients. Fifteen batch experiments were carried out with three central points, and three operating factors of current density (X_1: 16–80 mA/cm^2), initial pH (X_2: 5–9) and electrolysis time (X_3: 10–30 min) were investigated (Table 3). Y is the predicted response or output.

The analysis of variance (ANOVA) and the statistical analysis of the experimental data were conducted with the Statgraphics Centurion XVII software. The interaction between the operating factors and the COD removal was obtained by ANOVA. The quality of the fit of the polynomial model was expressed by the coefficient of determination (R^2) and adjusted R^2. Fisher's F-test was also used to check the statistical significance in the same software; a large F-value indicates high significance for the corresponding term. Based on the *p*-value, the model terms were selected or rejected (*p*-value $\ll 0.05$ shows that the model terms are significant at 95% confidence level).

Table 2 | Experimental original and coded factors and levels for EC process

	Coded factor		
Factor	**−1**	**0**	**1**
X_1: Current density (mA/cm^2)	16	48	80
X_2: pH	5	7	9
X_3: Time (min)	10	20	30

Table 3 | Experimental runs and the removal efficiencies of COD in EC process using Al and Fe electrodes

				Y_1: COD removal for Al electrode (%)		Y_2: COD removal for Fe electrode (%)	
Run	**X_1:j mA/cm^2**	**X_2:pH –**	**X_3:time min**	**Exp.**	**Pred.**	**Exp.**	**Pred.**
1	16	5	20	62.02	60.97	30.49	32.50
2	80	5	20	62.02	59.63	53.97	56.09
3	16	9	20	43.75	46.14	49.35	47.23
4	80	9	20	59.28	60.33	56.03	54.01
5	16	7	10	43.11	42.29	30.92	34.31
6	80	7	10	51.59	52.10	59.62	62.91
7	16	7	30	54.49	53.97	60.30	57.02
8	80	7	30	56.20	57.01	62.19	58.79
9	48	5	10	55.17	57.04	55.42	50.01
10	48	9	10	44.82	43.25	59.36	58.09
11	48	5	30	57.05	58.62	59.79	61.06
12	48	9	30	60.13	58.27	60.22	65.63
13	48	7	20	59.28	58.84	59.62	59.51
14	48	7	20	58.48	58.84	59.28	59.51
15	48	7	20	58.76	58.84	59.65	59.51

Total operating cost

In the EC process, the operating cost is affected by several important factors such as electrical energy cost, electrode types, maintenance, produced sludge treatment and disposal, hand labor and chemical product costs. It may be stated that the most important operating parameters are electrical energy and electrode costs in EC. Therefore, only electrical energy consumption (ENC: kWh/m^3) and electrode consumption (ELC: kg/m^3) were considered to evaluate the total operating cost (TOC: €/m^3) for the treated biodiesel wastewater effluent (Taheri *et al.* 2013; Kobya *et al.* 2016).

$$ENC = \frac{U \times I \times t}{V} \quad (18)$$

$$ELC = \frac{I \times t \times M}{Z \times F \times V} \quad (19)$$

$$TOC = aENC + bELC \quad (20)$$

where U is voltage (V), I is the current (A), t is the EC electrolysis time (h), V is the treated wastewater volume (m^3), M is the molecular mass of the aluminum and iron electrodes (29.98 g/mol and 55.84 g/mol), Z is the number of electrons transferred (Z = 3 for aluminum and iron), and F is the Faraday constant (96,487 C/mol) (Khandegar & Saroha 2013).

Downloaded from http://iwaponline.com/wst/article-pdf/79/12/2366/620291/wst079122366.pdf
by guest

RESULTS AND DISCUSSION

Evaluation of experimental design results and model development

The experimental design matrix including the actual and predicted results for COD removal efficiencies is shown in Table 3. The full quadratic regression model for COD removal in terms of the coded parameters is given in Equations (21) and (22). Positive signs and negative signs of the coefficients in Equations (21) and (22) show the antagonistic and synergistic effects, respectively (Bajpai *et al.* 2012). It can be stated that the COD removal efficiencies increased with an increase in the current density and electrolysis time with the positive sign of the coefficients and decreased with a decrease in the initial pH value with the negative sign of the coefficients for the Al electrodes (Equation (21)). On the other hand, the equation that was obtained for the Fe electrodes shows that all operating parameters had positive effects on COD removal efficiencies (Equation (22)).

$$Y_1 = 76.692 + 0.0170865\,X_1 - 9.57194\,X_2 + 1.48656\,X_3 - 0.00245433\,X_1^2 + 0.0606536\,X_1X_2 - 0.00528162\,X_1X_3 + 0.109686\,X_2^2 + 0.167892\,X_2X_3 - 0.0498349\,X_3^2 \quad (21)$$

$$Y_2 = -70{,}7609 + 1{,}93615\,X_1 + 17{,}1778\,X_2 + 0{,}781148\,X_3 - 0{,}0085433\,X_1^2 - 0{,}0656668\,X_1X_2 - 0{,}020953\,X_1X_3 - 0{,}826297\,X_2^2 - 0{,}043845\,X_2X_3 + 0{,}0249074\,X_3^2 \quad (22)$$

The results of ANOVA for the COD removals using Al and Fe electrodes are presented in Table 4. The very high correlation coefficient (R^2) values of 95.20% and 91.43% confirm the high accuracy of the model equations for all operating parameters in the EC process using Al and Fe electrodes, respectively. On the other hand, relatively high R^2 between the experimental results and model-predicted values verified the fit of the quadratic equations. A closer value of R^2 and Adj.R^2 confirms an appreciable interaction between the independent variables (the differences between R^2 and Adj.R^2 are lower than 20%). The *p*-values were applied for the significance of each model. It can be stated that the model terms are significant or highly significant if the *p*-values are found to be smaller than 0.05 or 0.0001, respectively. The sum of square (SS) of residual error was found to be very low in comparison to the total SS for the COD responses for the Al and Fe electrodes, which confirms the high reliability of the fitted second order polynomial models with a 95% confidence interval. The F-values of the model 11.032 and 5.924 for the Al and Fe electrodes respectively indicate that the model was significant (Table 4).

Statistical analysis and effects of operating factors on the COD removal efficiencies

Table 5 presents the ANOVA results of the operating parameters of the predicted response surface quadratic model and other statistical parameters of the COD removal values for the Al and Fe electrodes. The linear coefficients of current density (X_1), initial pH (X_2) and electrolysis time (X_3) had significant effects on COD removal efficiency for Al electrodes (*p*-value <0.05). The current density's second order terms (X_3^2) and the quadratic terms of X_1X_2 and X_2X_3 also had significant effects on the removal of COD for the Al electrodes (*p*-value: 0.0096, 0.0214 and 0.0356, respectively). In terms of the Fe electrodes, the results of ANOVA indicated that only current density (X_1), electrolysis time (X_3), the second order term of current density (X_1^2) and the quadratic term of X_1X_3 had significant effects on the removal of COD.

The response curve graphs of the quadratic models were presented for Al and Fe electrodes in Figure 2. Figure 2(a)–2(c) show the effects of current density, initial pH and electrolysis time on the removal efficiency of COD for the Al electrode. As can be seen from Figure 2(a), a slight increase in COD removal efficiency was observed with an increase in the current density. It can be shown from Figure 2(b) that at first the COD removal efficiency increases with increased current density and electrolysis time for the Al electrode. However, as the current density and electrolysis time reached maximum values, removal efficiency of COD no longer improved. As can be seen

Table 4 | ANOVA of the predicted response surface quadratic model

Model	R^2	Adj.R^2	Sum of squares (SS)	SS of the residual error	Mean square	F-value	*p*-value (Prob. > F)
Y_1	95.20	86.58	576.78	27.65	61.01	11.032	0.008302
Y_2	91.43	75.99	1,441.34	123.58	146.42	5.924	0.032189

Downloaded from http://iwaponline.com/wst/article-pdf/79/12/2366/620291/wst079122366.pdf
by guest

Table 5 | ANOVA results for the response surface quadratic model of COD removals

	Source	Sum of squares	Df	Mean square	F-ratio	*p*-value
Y_1: COD removal for Al electrode	X_1	82.598	1	82.598	14.93	0.0118*
	X_2	99.9291	1	99.9291	18.07	0.0081*
	X_3	137.708	1	137.708	24.90	0.0041*
	X_1^2	23.322	1	23.322	4.22	0.0952
	X_1X_2	60.2743	1	60.2743	10.90	0.0214*
	X_1X_3	11.426	1	11.426	2.07	0.2101
	X_2^2	0.71075	1	0.71075	0.13	0.7346
	X_2X_3	45.1002	1	45.1002	8.15	0.0356*
	X_3^2	91.6991	1	91.6991	16.58	0.0096*
	Total error	27.6532	5	5.53064		
	Total (corr.)	576.781	14			
Y_2: COD removal for Fe electrode	X_1	461.176	1	461.176	18.66	0.0076*
	X_2	79.9575	1	79.9575	3.24	0.1320
	X_3	172.82	1	172.82	6.99	0.0457*
	X_1^2	282.585	1	282.585	11.43	0.0196*
	X_1X_2	70.6499	1	70.6499	2.86	0.1517
	X_1X_3	179.825	1	179.825	7.28	0.0429*
	X_2^2	40.3357	1	40.3357	1.63	0.2575
	X_2X_3	3.07581	1	3.07581	0.12	0.7386
	X_3^2	22.9062	1	22.9062	0.93	0.3799
	Total error	123.577	5	24.7154		
	Total (corr.)	1,441.34	14			

*significant terms (*p*-value <0.05).

from Figure 2(c), the initial pH has an adverse effect on COD removal efficiencies and the increase in initial pH led to a decrease in COD removal. Figure 2(d)–2(f) show the effect of operating parameters on COD removal efficiency for the Fe electrode. Figure 2(d) indicates the effect of current density and initial pH on COD removal, and it was observed that high COD removals were obtained at high current density values. As can be seen from Figure 2(d) and 2(f), initial pH significant effect on COD removal. Figure 2(e) shows the interaction of current density and electrolysis time. It can be said that the electrolysis time has a positive significant effect on COD removal efficiencies and the COD removal efficiency increased slightly with an increase in electrolysis time.

In order to accurately determine the optimum operating conditions for maximum COD removal, response surface and desirability functions were used. The optimized conditions that were attained from the optimization of COD removal values for the Al and Fe electrodes are given in Table 6. The optimum operating conditions were 43 mA/cm^2, 5, and 21 min for current density, initial pH and electrolysis time respectively for Al electrodes. Under the optimized conditions, the optimum model prediction value of COD removal was 62.9%. In order to control the accuracy of the model-predicted value, additional EC experiments were performed; 62.7% COD removal efficiency was achieved and COD concentration was determined to be 11,025 mg/L after the EC process using Al electrodes. On the other hand, the optimum conditions for the Fe electrode were 47 mA/cm^2, 7.7 and 30 min for current density, initial time and electrolysis time, respectively. The optimum COD removals were determined as 67.1% and 63.4% by model prediction and additional experiments, respectively. It was noted that COD concentration decreased to 10,815 mg/L from 29,550 mg/L after the EC treatment with Fe electrodes.

The oil & grease, total phosphorus, orthophosphate and TSS removal efficiencies were found to be above 86.7% under the optimum conditions determined for the removal of COD for both electrode types. Direct discharge limits to a receiving water body for biodiesel wastewater in Turkey are 400 mg/L COD, 200 mg/L TSS, 20 mg/L oil & grease and 2 mg/L orthophosphate (Ministry of Environment and Urbanization, MoEU). According to the removal results obtained at the optimized conditions, the biodiesel wastewater direct discharge limits (COD must be <400 mg/L) or discharge limit standards for municipal sewage systems (COD must be <4,000 mg/L) have not been met based on the standards in the Water Pollution Control Regulation of Turkey, as the COD concentrations of treated wastewater were found to be above these discharge standards.

Downloaded from http://iwaponline.com/wst/article-pdf/79/12/2366/620291/wst079122366.pdf
by guest

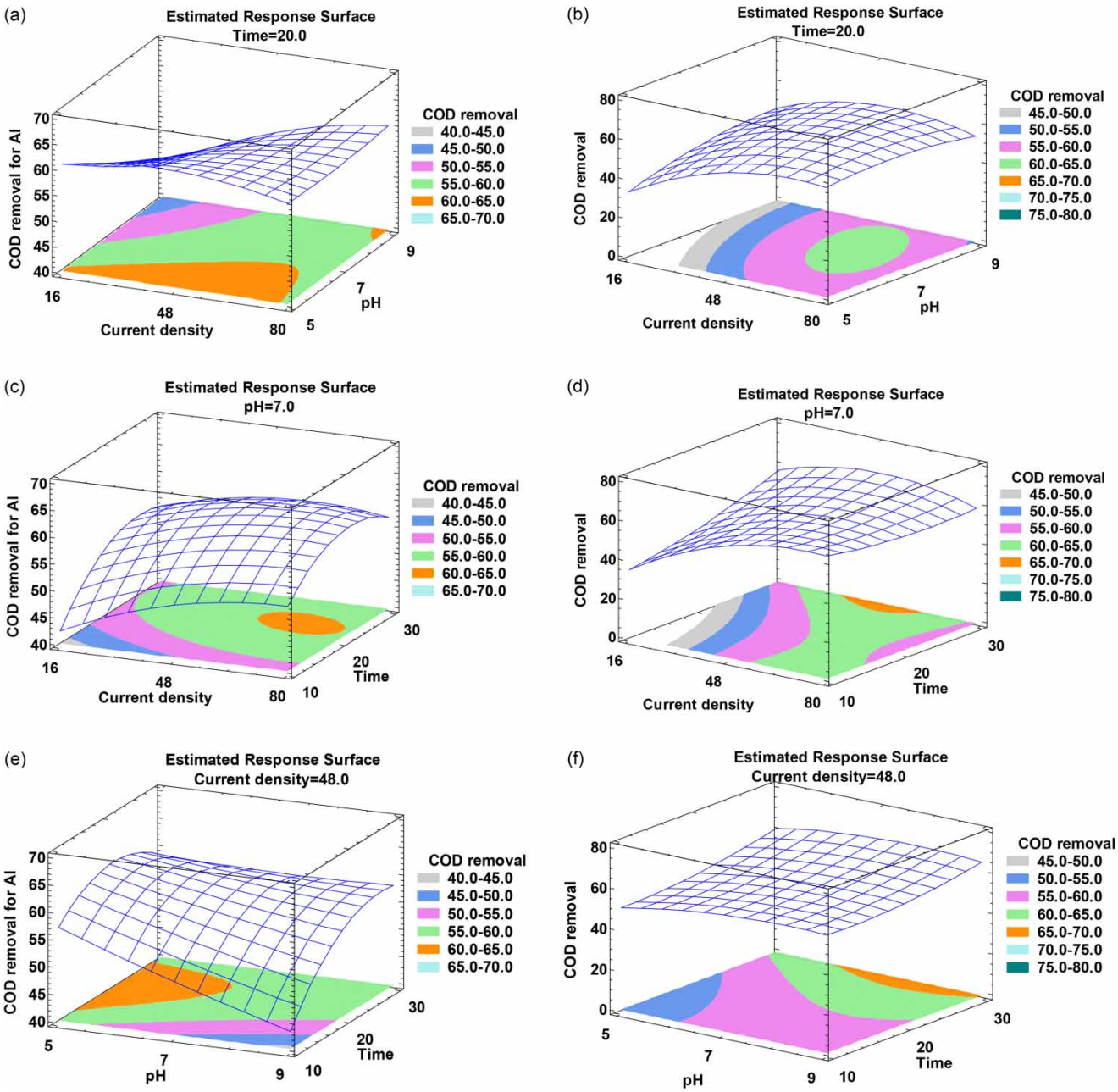


Figure 2 | Response surface graphs for COD removal efficiencies for Al electrode (a)–(c) and Fe electrode (d)–(f) in EC process.

Therefore, further advanced treatment processes should be investigated in order to meet the discharge limits for biodiesel wastewater.

Economic evaluation

Energy consumptions and mass loss of electrodes are the main costs of the EC process in wastewater treatment. Chemical consumption only results from the pH adjustment of wastewater before the EC process. The operational costs were found to be 6.43 €/m^3 and 7.01 €/m^3 for aluminum and iron electrodes, respectively, at optimum operating conditions.

Sludge characterization

Under the optimum conditions for Al and Fe electrodes, the sludge SEM and FT-IR analyses were performed to

Downloaded from http://iwaponline.com/wst/article-pdf/79/12/2366/620291/wst079122366.pdf
by guest

Table 6 | Optimum operating conditions and removal efficiencies for Al and Fe electrodes

Factor	Y_1: COD removal for Al electrode	Y_2: COD removal for Fe electrode
Current density (mA/cm^2)	43	47
Initial pH	5	7.7
Reaction time (min)	21	30
Model prediction results (%)	62.9	67.1
Experimental results (%)	62.7	63.4
Other removed parameters at optimized conditions for COD removal		
Oil & grease removal (%)	89.9	90.8
Total phosphorus (%)	98.9	98.5
Orthophosphate (%)	99.5	97.6
TSS (%)	86.7	89.8

identify the sludge characterization. Figure 3 shows the SEM images for aluminum and iron sludge. As can be seen in Figure 3(a)–3(c), aluminum sludge is more porous as compared to iron sludge (Figure 3(d)–3(f)) and the particle size of iron sludge remains smaller than aluminum sludge.

From the FT-IR spectra of produced sludges (Figure 4), the band in the region of 2,925–2,855 cm^{-1} represented CH_3 alkane stretching for both sludge samples, which was attributed to fatty acid methyl esters from the transesterification of biodiesel wastewater used oil. Peaks at the 1,742.99 and 1,741.52 cm^{-1} band of both Al and Fe sludge samples are likely to be attributed to methyl ester (COOMe) and free faty acids (Ngamlerdpokin *et al.* 2011). On the other hand, the band in the region of 2,924–3,378 cm^{-1} can be associated with the O-H stretching which is associated with adsorbed water (Guzman *et al.* 2016). The peaks between the 1,631.63 and 1,547.47 cm^{-1} bands of both sludge samples correspond to γ(OH) water bending vibration and hydroxyl bending (Parga *et al.* 2005). The bands at 1,374.77 and 1,467.40 cm^{-1} can be attributed to Al-O-H bending. On the other hand, 1,020.24 and 1,242.04 cm^{-1} bands were associated with carbonyl groups or carbohydrate bending vibrations (Anand *et al.* 2014). The FT-IR results for sludges indicate that pollutants in the biodiesel wastewater including oil & grease and other pollutants were removed successfully, as the peaks at 2,925–2,855 cm^{-1}, 1,742.99–1,741.52 cm^{-1} and 1,020.24–1,242.04 cm^{-1} were associated with fatty acid methyl esters, methyl ester (COOMe) and free fatty acids and carbonyl groups or carbohydrate bending vibrations, respectively.

Comparison of literature data with obtained results

Due to the high amount of wastewater (containing high COD) produced during biodiesel production, biodiesel wastewater should be treated effectively. Although the EC process is one of the attractive and efficient treatment methods, there are only a few studies that have investigated the treatment of biodiesel wastewater by the EC process so far. Chavalparit & Ongwandee (2009) investigated the EC process using aluminum and graphite electrodes for the biodiesel wastewater treatment. The authors optimized the operating conditions using the Box-Behnken design and RSM. The optimum operating conditions were determined as 6.06 of pH, 18.2 V of applied voltage and 23.5 min of reaction time. In these operating conditions, COD, oil & grease and suspended solids removal efficiencies were 55.43%, 98.42% and 96.59%, respectively. The operating cost was also investigated, and it was found that 5.57 kWh/m^3 of power would be required for the treatment of biodiesel wastewater at the optimum operating conditions. On the other hand, Srirangsan *et al.* (2009) examined the treatment of biodiesel wastewater by the EC process using different types of electrode pairs including aluminum, iron and carbon (Fe-Fe, Fe-C, Al-Al, Al-C and C-C). At the end of the optimization study, the process was efficient at 6, 8.32 mA/cm^2 and 25 min for the pH, current density and reaction time for the pair of Al-C. COD, oil & grease and suspended solids removal efficiencies were found as 55.4%, 97.8% and 96.9%, respectively. Ngamlerdpokin *et al.* (2011) also compared the chemical coagulation and electrocoagulation processes for remediation of biodiesel wastewater. In their study, the free fatty acids in biodiesel wastewater were chemically removed from the wastewater using mineral acids, H_2SO_4 and HCl at 2.5 pH and 7 min, and 38.94% COD, 76.32% biochemical oxygen demand (BOD_5) and 99.36% of oil & grease was removed. After the pretreatment, chemical coagulation and EC were investigated, and both treatment methods were found to be effective. In the chemical coagulation, 97.5% COD, 97.2% BOD_5 and 98.2% oil & grease removal efficiencies were obtained at the optimum conditions (6 pH and 2 g/L of $Al_2(SO_4)_3$). The optimum conditions were found to be 7.4 pH, 13 mA/cm^2 current density and 4 h reaction time in the EC process. The COD, BOD_5 and oil & grease removal efficiencies were 99.6%, 91.5% and 98.7% in the EC process using Fe electrodes. Although a lower cost was obtained by the chemical coagulation

Downloaded from http://iwaponline.com/wst/article-pdf/79/12/2366/620291/wst079122366.pdf
by guest

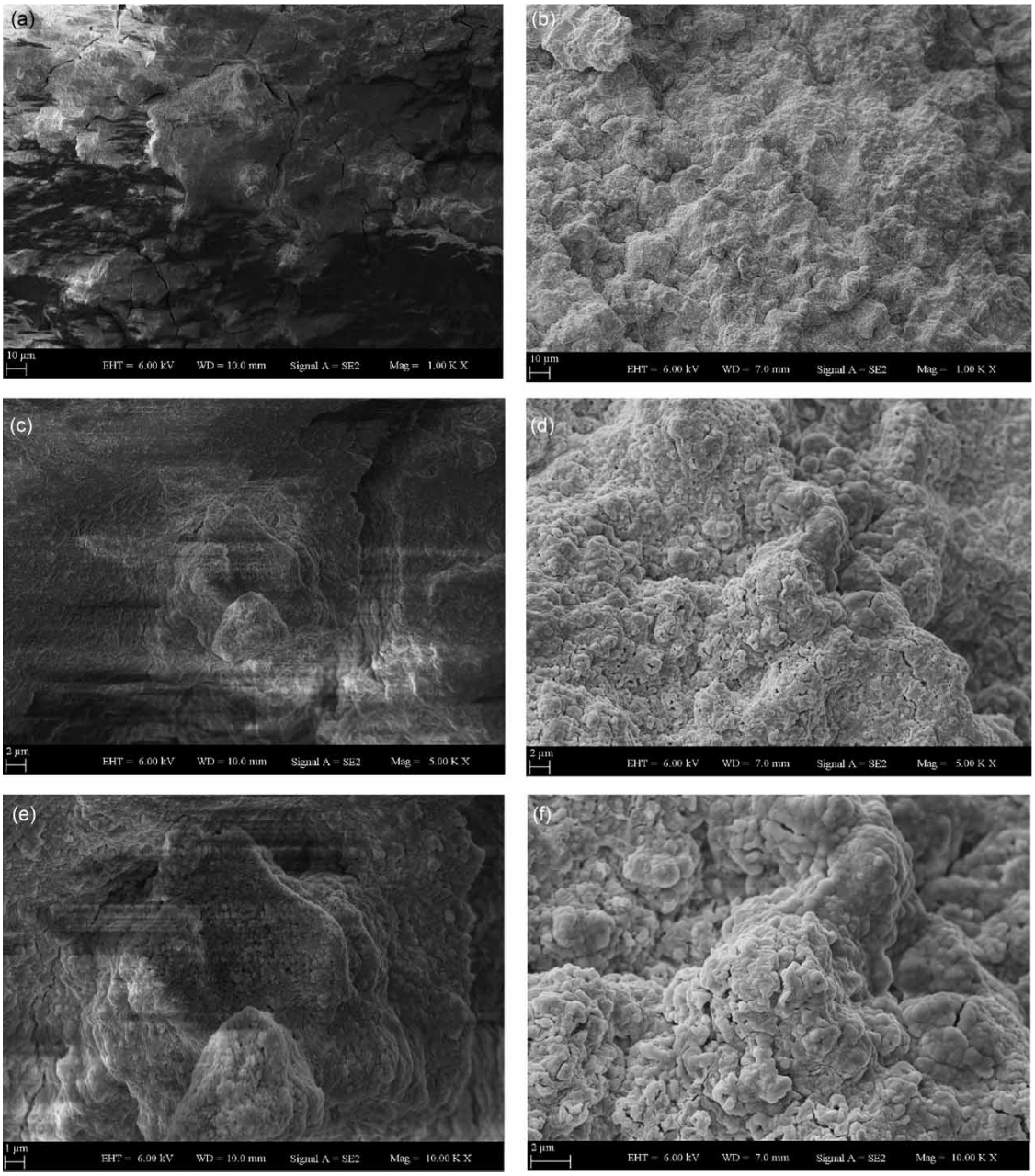


Figure 3 | SEM results of waste sludge at optimum conditions ((a) 1 K, (b) 5 K, (c) 10 K for Al and (d) 1 K, (e) 5 K, (f) 10 K for Fe).

process, the EC process provided a better effluent quality in terms of the investigated parameters. In this study, 62.7% and 63.4% COD removal efficiencies were found at the optimum operating conditions for the Al-Al and Fe-Fe electrodes (43 mA/cm^2 for current density, 5 for initial pH, and 21 min for electrolysis time for Al electrode and 47 mA/cm^2, 7.7 and 30 min for current density, initial pH and electrolysis time for Fe electrode), respectively. The operating cost was determined as 6.43 €/m^3 and 7.01 €/m^3 for the Al and Fe electrodes, respectively. It may be stated that the results of this study and the previous studies show that the treatment of biodiesel wastewater by the EC process is suitable, and the EC process is a cost-effective treatment process. However, further treatment methods such as electro-oxidation using different electrodes and peroxy-electrocoagulation should be investigated to achieve the local discharge standards.

Downloaded from http://iwaponline.com/wst/article-pdf/79/12/2366/620291/wst079122366.pdf
by guest

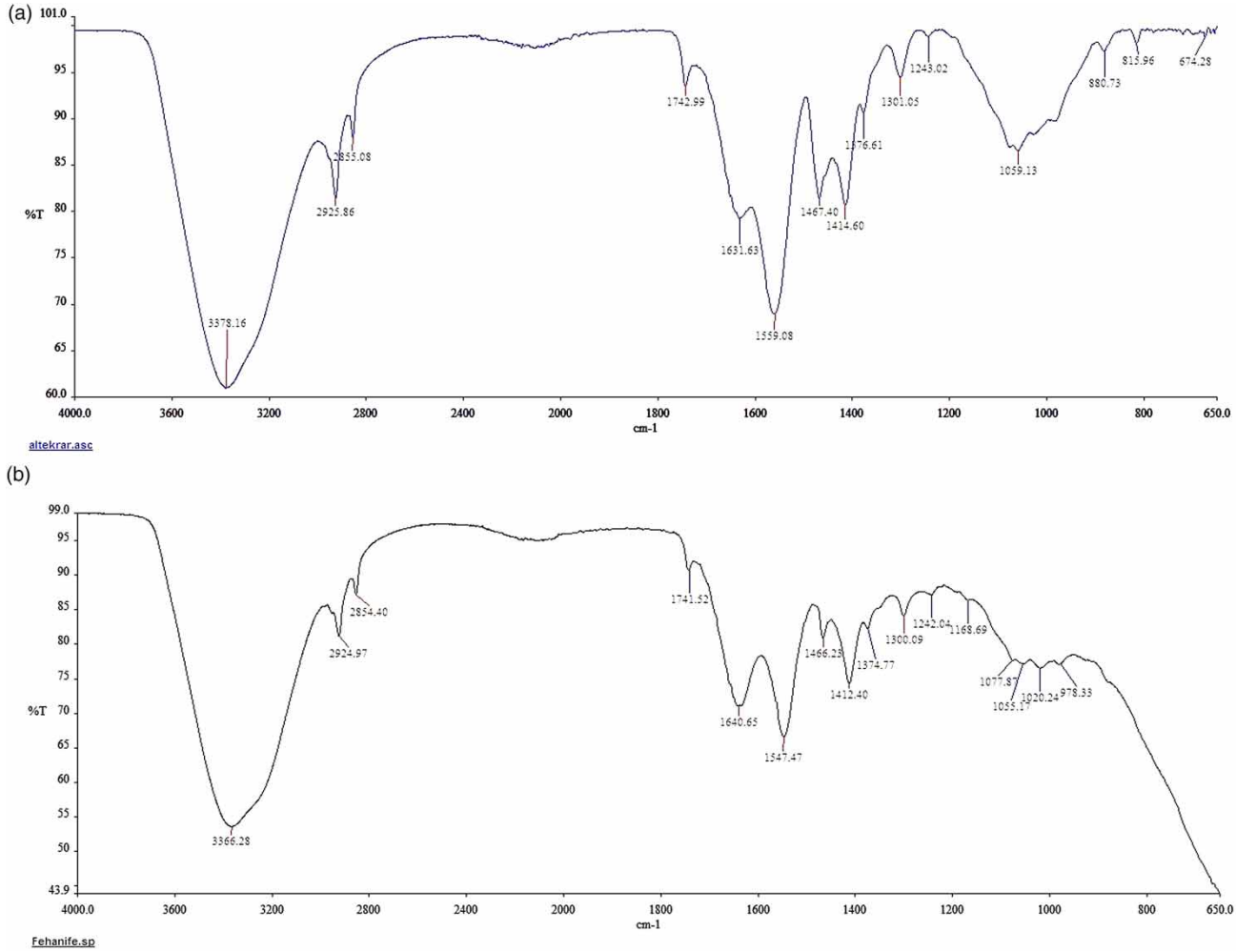


Figure 4 | FT-IR spectra of waste sludge for Al (a) and Fe (b) electrodes under the optimized conditions.

CONCLUSION

This study focused on the treatment of biodiesel wastewater by the EC process using Al and Fe electrodes to remove COD, oil & grease, total phosphorus, orthophosphate and TSS from wastewater. For this purpose, laboratory experiments were performed using the CCD for the optimization of process parameters including current density, initial pH and electrolysis time, and RSM was used for the process optimization of EC. It was noted that the optimization studies were only performed for COD removal. The ANOVA results show that the high R^2 (>91.43) ensures a satisfactory adjustment of the second-order regression model with the experimental data. The optimization of the model provides the optimum conditions for the removal of COD using Al electrodes at a current density of 43 mA/cm^2, initial pH of 5 and 21 minutes of electrolysis time. The removal efficiencies of COD, oil & grease, total phosphorus, orthophosphate and TSS were found to be 62.7%, 89.9%, 98.9%, 99.5% and 86.7% at the optimized conditions, respectively. On the other hand, under the optimum operating conditions for the removal of COD using the Fe electrodes (current density: 47 mA/cm^2, initial pH: 7.7 and electrolysis time: 30 minutes), the removal efficiencies were found to be almost equal to the results that were obtained using the Al electrodes. The total operational cost was found to be 6.43 €/m^3 and 7.01 €/m^3 for the aluminum and iron electrodes, respectively. Consequently, the obtained results indicate that excellent removal for oil & grease, total phosphorus, orthophosphorus and TSS can be achieved by the EC process and RSM is a powerful technique to optimize the operating parameters.

Downloaded from http://iwaponline.com/wst/article-pdf/79/12/2366/620291/wst079122366.pdf
by guest

REFERENCES

Abbaszaadeh, A., Ghobadian, B., Omidkhah, M. R. & Najafi, G. 2012 Current biodiesel production technologies: a comparative review. *Energy Conversion and Management* **63**, 138–148.

Abou-Shanab, R. A., Hwang, J.-H., Cho, Y., Min, B. & Jeon, B.-H. 2011 Characterization of microalgal species isolated from fresh water bodies as a potential source for biodiesel production. *Applied Energy* **88** (10), 3300–3306.

Al-Qodah, Z. & Al-Shannag, M. 2017 Heavy metal ions removal from wastewater using electrocoagulation processes: a comprehensive review. *Separation Science and Technology* **52** (17), 2649–2676.

Al-Shannag, M., Al-Qodah, Z., Bani-Melhem, K., Qtaishat, M. R. & Alkasrawi, M. 2015 Heavy metal ions removal from metal plating wastewater using electrocoagulation: kinetic study and process performance. *Chemical Engineering Journal* **260**, 749–756.

Anand, M. V., Srivastava, V. C., Singh, S., Bhatnagar, R. & Mall, I. D. 2014 Electrochemical treatment of alkali decrement wastewater containing terephthalic acid using iron electrodes. *Journal of the Taiwan Institute of Chemical Engineers* **45** (3), 908–913.

APHA (American Public Health Association) 2005 *Standard Methods for the Examination of Water and Wastewater*, 21st edn. APHA-AWWA-WEF, Washington, DC.

Bajpai, S., Gupta, S. K., Dey, A., Jha, M. K., Bajpai, V., Joshi, S. & Gupta, A. 2012 Application of Central Composite Design approach for removal of chromium (VI) from aqueous solution using weakly anionic resin: modeling, optimization, and study of interactive variables. *Journal of Hazardous Materials* **227**, 436–444.

Barnwal, B. K. & Sharma, M. P. 2005 Prospects of biodiesel production from vegetable oils in India. *Renewable and Sustainable Energy Reviews* **9** (4), 363–378.

Butler, E., Hung, Y. T., Yeh, R. Y. L. & Al Ahmad, M. S. 2011 Electrocoagulation in wastewater treatment. *Water* **3** (2), 495–525.

Chavalparit, O. & Ongwandee, M. 2009 Optimizing electrocoagulation process for the treatment of biodiesel wastewater using response surface methodology. *Journal of Environmental Sciences* **21** (11), 1491–1496.

Chen, Y., Xiao, B., Chang, J., Fu, Y., Lv, P. & Wang, X. 2009 Synthesis of biodiesel from waste cooking oil using immobilized lipase in fixed bed reactor. *Energy Conversion and Management* **50** (3), 668–673.

Daud, N. M., Abdullah, S. R. S., Hasan, H. A. & Yaakob, Z. 2015 Production of biodiesel and its wastewater treatment technologies: a review. *Process Safety and Environmental Protection* **94**, 487–508.

Demirbas, A. 2009 Progress and recent trends in biodiesel fuels. *Energy Conversion and Management* **50** (1), 14–34.

Emamjomeh, M. M. & Sivakumar, M. 2009 Review of pollutants removed by electrocoagulation and electrocoagulation/flotation processes. *Journal of Environmental Management* **90** (5), 1663–1679.

Ganapathy, T., Murugesan, K. A. & Gakkhar, R. 2009 Performance optimization of Jatropha biodiesel engine model using Taguchi approach. *Applied Energy* **86** (11), 2476–2486.

Guzman, A., Nava, J. L., Coreno, O., Rodriguez, I. & Gutierrez, S. 2016 Arsenic and fluoride removal from groundwater by electrocoagulation using a continuous filter-press reactor. *Chemosphere* **144**, 2113–2120.

Jaruwat, P., Kongjao, S. & Hunsom, M. 2010 Management of biodiesel wastewater by the combined processes of chemical recovery and electrochemical treatment. *Energy Conversion and Management* **51** (3), 531–537.

Karatay, S. E. & Dönmez, G. 2011 Microbial oil production from thermophile cyanobacteria for biodiesel production. *Applied Energy* **88** (11), 3632–3635.

Khandegar, V. & Saroha, A. K. 2013 Electrocoagulation for the treatment of textile industry effluent – a review. *Journal of Environmental Management* **128**, 949–963.

Kobya, M., Gengec, E. & Demirbas, E. 2016 Operating parameters and costs assessments of a real dyehouse wastewater effluent treated by a continuous electrocoagulation process. *Chemical Engineering and Processing* **101**, 87–100.

Kumjadpai, S., Ngamlerdpokin, K., Chatanon, P., Lertsathitphongs, P. & Hunsom, M. 2011 Management of fatty acid methyl ester (FAME) wastewater by a combined two stage chemical recovery and coagulation process. *The Canadian Journal of Chemical Engineering* **89** (2), 369–376.

Liu, H., Zhao, X. & Qu, J. 2010 Electrocoagulation in water treatment. In: *Electrochemistry for the Environment* (C. Comninellis & G Chen, eds), pp. 245–262. Springer, Dordrecht, The Netherlands.

Marchetti, J., Miguel, V. & Errazu, A. 2008 Techno-economic study of different alternatives for biodiesel production. *Fuel Processing Technology* **89** (8), 740–748.

Mathews, J. A. 2008 Carbon-negative biofuels. *Energy Policy* **36** (3), 940–945.

Ngamlerdpokin, K., Kumjadpai, S., Chatanon, P., Tungmanee, U., Chuenchuanchom, S., Jaruwat, P., Lertsathitphongs, P. & Hunsom, M. 2011 Remediation of biodiesel wastewater by chemical-and electro-coagulation: a comparative study. *Journal of Environmental Management* **92** (10), 2454–2460.

Omar, W. N. N. W. & Amin, N. A. S. 2011 Optimization of heterogeneous biodiesel production from waste cooking palm oil via response surface methodology. *Biomass and Bioenergy* **35** (3), 1329–1338.

Parga, J. R., Cocke, D. L., Valenzuela, J. L., Gomes, J. A., Kesmez, M., Irwin, G., Moreno, H. & Weir, M. 2005 Arsenic removal via electrocoagulation from heavy metal contaminated groundwater in La Comarca Lagunera Mexico. *Journal of Hazardous Materials* **124** (1–3), 247–254.

Pitakpoolsil, W. & Hunsom, M. 2013 Adsorption of pollutants from biodiesel wastewater using chitosan flakes. *Journal of the Taiwan Institute of Chemical Engineers* **44** (6), 963–971.

Ramírez, X. M. V., Mejía, G. M. H., López, K. V. P., Vásquez, G. R. & Sepúlveda, J. M. M. 2012 Wastewater treatment from biodiesel production via a coupled photo-Fenton–aerobic sequential batch reactor (SBR) system. *Water Science and Technology* **66** (4), 824–830.

Downloaded from http://iwaponline.com/wst/article-pdf/79/12/2366/620291/wst079122366.pdf
by guest

Rattanapan, C., Sawain, A., Suksaroj, T. & Suksaroj, C. 2011 Enhanced efficiency of dissolved air flotation for biodiesel wastewater treatment by acidification and coagulation processes. *Desalination* **280** (1–3), 370–377.

Sandhwar, V. K. & Prasad, B. 2018 Comparison of electrocoagulation, peroxi-electrocoagulation and peroxi-coagulation processes for treatment of simulated purified terephthalic acid wastewater: optimization, sludge and kinetic analysis. *Korean Journal of Chemical Engineering* **35** (4), 909–921.

Siddiquee, M. N. & Rohani, S. 2011 Lipid extraction and biodiesel production from municipal sewage sludges: a review. *Renewable and Sustainable Energy Reviews* **15** (2), 1067–1072.

Srirangsan, A., Ongwandee, M. & Chavalparit, O. 2009 Treatment of biodiesel wastewater by electrocoagulation process. *Environment Asia* **2** (2), 15–19.

Suehara, K.-i., Kawamoto, Y., Fujii, E., Kohda, J., Nakano, Y. & Yano, T. 2005 Biological treatment of wastewater discharged from biodiesel fuel production plant with alkali-catalyzed transesterification. *Journal of Bioscience and Bioengineering* **100** (4), 437–442.

Sukkasem, C., Laehlah, S., Hniman, A., O-Thong, S., Boonsawang, P., Rarngnarong, A., Nisoa, M. & Kirdtongmee, P. 2011 Upflow bio-filter circuit (UBFC): biocatalyst microbial fuel cell (MFC) configuration and application to biodiesel wastewater treatment. *Bioresource Technology* **102** (22), 10363–10370.

Taheri, M., Moghaddam, M. R. A. & Arami, M. 2013 Techno-economical optimization of Reactive Blue 19 removal by combined electrocoagulation/coagulation process through MOPSO using RSM and ANFIS models. *Journal of Environmental Management* **128**, 798–806.

Talebian-Kiakalaieh, A., Amin, N. A. S. & Mazaheri, H. 2013 A review on novel processes of biodiesel production from waste cooking oil. *Applied Energy* **104**, 683–710.

Tan, K., Lee, K. & Mohamed, A. 2011 Potential of waste palm cooking oil for catalyst-free biodiesel production. *Energy* **36** (4), 2085–2088.

Un, U. T., Koparal, A. S. & Ogutveren, U. B. 2009 Electrocoagulation of vegetable oil refinery wastewater using aluminum electrodes. *Journal of Environmental Management* **90** (1), 428–433.

Vyas, A. P., Verma, J. L. & Subrahmanyam, N. 2010 A review on FAME production processes. *Fuel* **89** (1), 1–9.

Xie, Q.-g., Taweepreda, W., Musikavong, C. & Suksaroj, C. 2011 Separation of oily sludge and glycerol from biodiesel processing waste by coagulation. *Songklanakarin Journal of Science & Technology* **33** (6), 699–703.

Yaakob, Z., Mohammad, M., Alherbawi, M., Alam, Z. & Sopian, K. 2013 Overview of the production of biodiesel from waste cooking oil. *Renewable and Sustainable Energy Reviews* **18**, 184–193.

First received 4 December 2018; accepted in revised form 4 July 2019. Available online 17 July 2019

Downloaded from http://iwaponline.com/wst/article-pdf/79/12/2366/620291/wst079122366.pdf
by guest